Observations of Aerosols and Trace Gases around the Chikushi Campus of Kyushu University

Wang, Zhe
Research Institute for Applied Mechanics, Kyushu University | Institute of Atmospheric Physics, Chinese Academy of Sciences

Uno, Itsushi
Research Institute for Applied Mechanics, Kyushu University : Professor

Osada, Kazuo
Graduate School of Environmental Studies, Nagoya University

Pan, Xiaole
Institute of Atmospheric Physics, Chinese Academy of Sciences

他

https://doi.org/10.15017/1924421

出版情報：九州大学応用力学研究所所報. 153, pp.113-129, 2017-09. Research Institute for Applied Mechanics, Kyushu University
バージョン：
権利関係：

Observations of Aerosols and Trace Gases around the Chikushi Campus of Kyushu University

Zhe WANG[*1, 2], Itsushi UNO[*1], Kazuo OSADA[*3], Xiaole PAN[*2], Shigekazu YAMAMOTO[*4] and Yugo KANAYA[*5]

E-mail of corresponding author: *uno@riam.kyushu-u.ac.jp*

(Received July 31, 2017)

Abstract

To better understand seasonal variations in the components of $PM_{2.5}$ and related trace gases, and the impacts of long-range transport from the Asian continent to Japan, we analyzed long-term, simultaneous observations of fine- and coarse-mode nitrate, related aerosol components (SO_4^{2-}, NH_4^+, BC, OC), and trace gases (CO, NH_3, HNO_3) around the Chikushi Campus of Kyushu University, Fukuoka (33.52°N, 130.47°E), from August 2014 to October 2015. Daily and monthly mean aerosol concentrations were analyzed to assess the main seasonal variation in pollution. We found that fine aerosols (fSO_4^{2-}, fNO_3^-, and fNH_4^+) explained most of the seasonal change in $PM_{2.5}$. Polarization optical particle counter measurements were useful for detecting the onset of dust transport from the Asian continent, and we observed high concentrations of coarse-mode NO_3^- (cNO_3^-) during dust period, which indicated the formation of dust nitrate during transport. We also analyzed diurnal variation in the basic aerosol components for different seasons, weekday/weekend effects (for CO, BC, and NH_3), and sensitivity on days with and without precipitation (for CO, BC, NH_3, $PM_{2.5}$, and PM_c). Observational data for HNO_3, fNO_3^-, and cNO_3^- demonstrated that cNO_3^- accounted for the largest proportion of total nitrate (defined as the sum of fNO_3^-, cNO_3^-, and HNO_3), constituting 40–55% of the total nitrate during the winter, whereas HNO_3 gas constituted approximately 40% of the total nitrate in summer and fNO_3^- peaked during the winter.

Keywords : *Aerosols, $PM_{2.5}$, PM_{10}, NH_3, simultaneous observations, weekend effects, washout process*

1. Introduction

Heavy anthropogenic pollution and natural mineral dust events cause significant environmental problems in East Asia [1,2]. Many intensive field studies have been performed to better understand the transport and chemical evolution of dust and anthropogenic aerosols over East Asia, such as the Aerosol Characterization Experiments over Asia (ACE-Asia) [3,4] and Transport and Chemical Evolution over the Pacific (TRACE-P) [5,6] studies. In addition to these field observations, several numerical transport models have been used to illustrate the long-range transport (LRT) of Asian dust during the springtime, such as the Chemical Weather Forecast System (CFORS) [7,8] and the Nested Air Quality Prediction Modeling System (NAQPMS) [9]. However, because both the ACE-Asia and TRACE-P studies were conducted in the spring, details about aerosol processes in other seasons are still not clear.

In recent years, severe anthropogenic aerosol pollution has become a critically important environmental issue in China because of rapid economic development and associated increases in emissions. Specific instances of severe pollution, such as the heavy pollution event in January 2013, usually occur in winter [10,11]. Therefore, it is imperative that observational and modeling studies of anthropogenic aerosols be conducted in East Asia during winter.

In terms of the chemical composition of aerosols during heavy pollution events, sulfate (SO_4^{2-}), an important component of anthropogenic aerosols, has received much attention. The first phase of the Model Inter-Comparison Study in Asia (MICS-Asia Phase I),

*1 Research Institute for Applied Mechanics, Kyushu Univ.
*2 Institute of Atmospheric Physics, Chinese Academy of Sciences, Beijing, China
*3 Graduate School of Environmental Studies, Nagoya Univ.
*4 Fukuoka Institute of Health and Environmental Sciences
*5 Japan Agency for Marine-Earth Science and Technology

which involved eight LRT models, revealed the importance of SO_2 and SO_4^{2-} LRT over East Asia [12]. However, since 2006, strict emissions control implementation in China led to a dramatic decrease in SO_2 concentrations [13]; since then, NO_3^- has become more prevalent, particularly in winter when low temperature is favorable for the formation of NO_3^- [14]. Few literature was available on the LRT of nitrate (NO_3^-) compared to SO_4^{2-}, as the atmospheric lifetime of NO_3^- is shorter than that of SO_4^{2-}, and NO_3^- is more difficult to measure accurately than SO_4^{2-} because of the thermal equilibrium between nitric acid (HNO_3) and ammonia (NH_3).

These facts demonstrate the necessity for high-time resolution and long-term (i.e., over different seasons) observations of aerosol components (including both SO_4^{2-} and NO_3^- as well as others) in different aerosol size bins, however, no such detailed long-term observational studies have been undertaken to date.

Since October 2013, we have been performing long-term simultaneous observations of aerosol components and related trace gases around the Chikushi Campus of Kyushu University, located in the suburbs of Fukuoka City (33.52°N, 130.47°E) [14–20]. Mass concentrations of particulate matter and SO_4^{2-} and NO_3^- in both fine mode and coarse mode were measured. In this paper, we report seasonal variation in atmospheric aerosols based on long-term observations at 1 h intervals from August 2014 to October 2015.

2. Methodology

In this section, we describe the instruments used to measure aerosol components and related gases around the Chikushi Campus. Fig. 1 shows the locations of observation sites along with NH_3 emission intensities [21]. Table 1 summarizes the instruments used to observe different chemical components, including time resolutions, observation periods, and aerosol diameter ranges.

2.1 Aerosol chemical speciation analysis

A continuous dichotomous aerosol chemical speciation analyzer (ACSA-12 Monitor; Kimoto Electric Co., Ltd., Osaka, Japan) was used to measure PM_{10} (particulate matter <10 μm in diameter) and $PM_{2.5}$ (particulate matter <2.5 μm in diameter) at high temporal resolution [22]. Specifically, particulate matter (PM) was collected on a Teflon (PTFE) filter. Hourly observations were conducted to monitor SO_4^{2-}, NO_3^-, optical black carbon (OBC), and water-soluble organic compounds (WSOC) from the rooftop (4F) of the

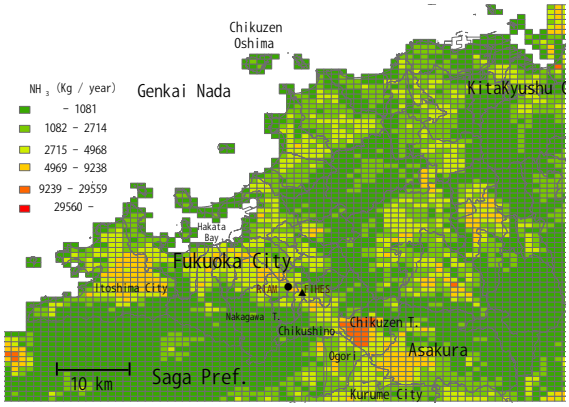

Fig. 1 Observation sites (RIAM and FIHES) and NH_3 emission intensity map (1 × 1 km resolution) [21].

Fukuoka Institute of Health and Environmental Science (FIHES; period: November 2013–September 2014 and December 2014–March 2015), the sixth floor of the G building (period: September 2014–December 2014), and the rooftop (6F) of RIAM (period: April 2016 to present) of the Chikushi Campus of Kyushu University. The horizontal distance from the FIHES site to the Chikushi Campus of Kyushu University site is about 5 km. Both sites are located in a suburban area of Fukuoka City. Anthropogenic activities were limited at both sites, and the sites had similar patterns in terms of air quality. Fig. 2a shows an *in-site* photo of the ACSA-12 instrument, situated on the RIAM roof.

Mass concentrations of PM were determined using the beta-ray absorption method. The ACSA-12 measured NO_3^- and WSOC by an ultraviolet absorption-photometric method and SO_4^{2-} by turbidimetry after the addition of $BaCl_2$ to form $BaSO_4$ and polyvinyl pyrrolidone as a stabilizer. Analyses were conducted within 2 h of sampling; therefore, the volatilization of particulate NH_4NO_3 after collection was

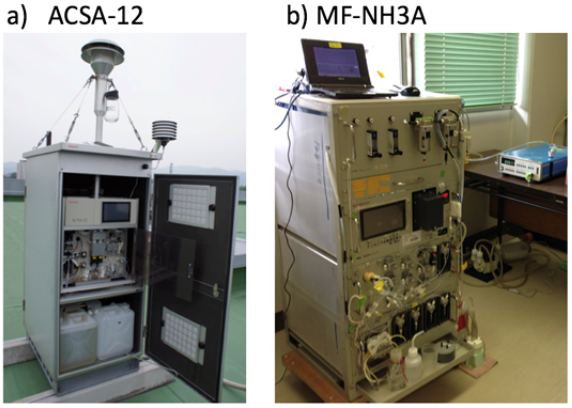

Fig. 2 Onsite view of (a) the ACSA-12 on the roof of RIAM and (b) MF-NH_3A and the control PC (situated in front of the regular optical particle counter and air pump) at 6F of G-building

Table 1 Summary of observation instruments.

Instrument & Time resolution	Period	Place	Aerosol diameters & Chemical components
ACSA-12 (aerosol chemical speciation analyzer) 1 h	2013.10.25–2014.9.11 2014.9.12–2015.3.24 2015.3.25–2016.3.29 2016.3.30+	FIHES Kyushu U. G Bldg 6F FIHES Kyushu U. RIAM Rf	Fine: Dp <2.5 μm Coarse: 2.5 < Dp < 10 μm $PM_{2.5}$, $PM_{2.5\text{-}10}$, SO_4^{2-}, NO_3^-, WSOC, OBC, ΔpH
NCSA-13 (nanoparticle chemical speciation analyzer) 1 h	2016.11.18+	Kyushu U. RIAM Rf	Fine: Dp <1.0 Coarse: 1 < Dp < 2.5 μm PM_1, $PM_{1–2.5}$, SO_4^{2-}, NO_3^-, WSOC, OBC, ΔpH
MF-NH_3A 1 h	2014.7.31–2015.10.19	Kyushu U. G Bldg 6F	Dp <2.0 μm NH_3 (gas), NH_4^+(p)
D-F (denuder-filter) pack Manual sampling and Ion chromatography 6 h to 3 days	2014.7.31–2015.10.19 (intensive observations) 2014.9.24–2014.10.9 2015.1.7–2015.1.17	Kyushu U. G Bldg 6F	Fine: Dp <1.9 μm Coarse: Dp >1.9 μm SO_4^{2-}, NO_3^-, NH_4^+, Cl^-, Oxl, Na^+, Ca^{2+}, K^+, Mg^{2+}, H^+, HNO_3 (gas)
POPC (polarization optical particle counter) 5 min	2013.12.1+	Kyushu U. RIAM 2F	Single aerosol particle with optical diameters: 0.5 < Dp < 10 μm
BC (MAAP5012) 1 h	2014.9.22–2016.7.26	Kyushu U. RIAM 2F	Black carbon (BC)
CO (Model 48) 1 h	2014.9.22–2016.3.8	Kyushu U. RIAM 2F	CO

considered minimal compared to the traditional filter pack observation method. The ACSA-12 was tested previously [20] and used to identify aerosol chemical compositions at Fukuoka [16–18]. The ACSA-12 measures both fine- and coarse-mode aerosols simultaneously and is important for mass budget studies.

2.2 NH_3 and NH_4^+ measurements

The behavior of NH_4^+ is important because it is a key counterpart for SO_4^{2-} and NO_3^-. Concentrations of gaseous NH_3 and aerosol NH_4^+ were measured using a semicontinuous microflow analytical system (MF-NH_3A; Kimoto Electric Co. Ltd.) [23] at the 6F G building of Chikushi Campus of Kyushu University. Atmospheric NH_x (NH_3 + NH_4^+) was dissolved in ultrapure water using a continuous air-water droplet sampler and quantified from the fluorescence signal (excitation, 360 nm; emission, 420 nm) of the *o*-phtalaldehyde-sulfite-NH_3 reaction product [24]. Two inlet lines were used to differentiate the total amount of NH_x from particulate NH_4^+ after the removal of gaseous NH_3 using a phosphoric acid–coated denuder from the sample air stream. The cutoff diameter of the inlet impactor was about 2 μm (which is smaller than the ACSA $PM_{2.5}$ cutoff). Thus, our simultaneous monitoring system enabled fully speciated measurements of secondary inorganic aerosols (SIA; SO_4^{2-}, NO_3^-, and NH_4^+). Fig. 2b shows the photo of the MF-NH_3A instrument.

2.3 Denuder-filter pack method

From August 2014 to October 2015, we conducted denuder-filter (D-F) pack measurements from the 6F floor balcony of the G building. An annular denuder-multistage filter sampling system was used for HNO_3 and size-segregated aerosol sampling. The sampling interval was 6–8 h for intensive observations and 1–2 days for regular observations. At the inlet, coarse-mode aerosols were removed using Nucleopore membrane filters (111114; Nomura Micro Science Co., Ltd., Atsugi, Japan; pore size = 8 μm), and then gas-phase HNO_3 was collected with an annular denuder (2000-30x242-3CSS; URG Co., Chapel Hill, NC, USA) coated with NaCl [25]. Fine-mode aerosols were collected with a PTFE filter (J100A047A; ADVANTEC, Tokyo, Japan; pore size = 1 μm), and a nylon filter (66509; Pall Co., Port Washington, NY, USA) captured volatized nitrates from the PTFE filter [26,27].

The sample flow rate was 16.7 L min^{-1} (1 atm, 25°C). Under these conditions, the aerodynamic diameter of the 50% cutoff for the Nuclepore filter was approximately 1.9 μm [28]. The samples were analyzed by ion chromatography (IC). Fine-mode aerosols (<1.9 μm in diameter) were underestimated by the D-F pack method compared to the ACSA $PM_{2.5}$ measurements, whereas coarse-mode aerosols (>1.9 μm, with no upper limit) were overestimated by the D-F pack method compared to the ACSA PM_c measurements (2.5–10 μm) because of differences in the cutoff diameters of the methods [20]. Details on the ACSA data comparison and validation have previously been reported [20]. Fig. 3 shows a schematic of the D-F measurement system.

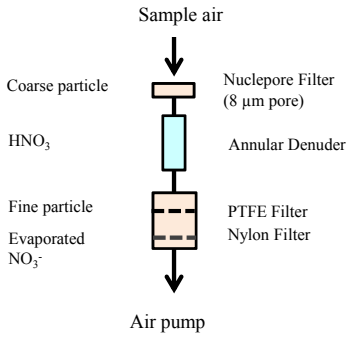

Fig. 3 Configuration of sampling lines for the denuder-filter (D-F) method.

2.4 Polarization optical particle counter measurements

The light polarization properties of atmospheric aerosol particles (0.5 μm < Dp < 10 μm) were measured using a newly developed polarization optical particle counter (POPC; YGK Corp., Yamanashi, Japan) from the top of a two-story building at RIAM Kyushu University. We installed a 3 m long vertical stainless steel tube through the roof of the building, and ambient air was drawn into the room at a flow rate of 13 L min^{-1} under laminar conditions. The loss of coarse-mode particles (Dp >2.5 μm) due to gravity settling was negligible. A detailed setup of the instrumentation is shown in Fig. 4.

The POPC uses a 780 nm linearly polarized laser source and measures both forward scattering and backward scattering intensities. Size of particle is determined on the basis of the forward scattering intensity, and two polarized components (s-polarized/p-polarized; polarization direction perpendicular and/or parallel to the plane of the scattering angle) of backward scattering are measured simultaneously. The depolarization ratio (DR; the fraction of s-polarized to the total backward scattering,

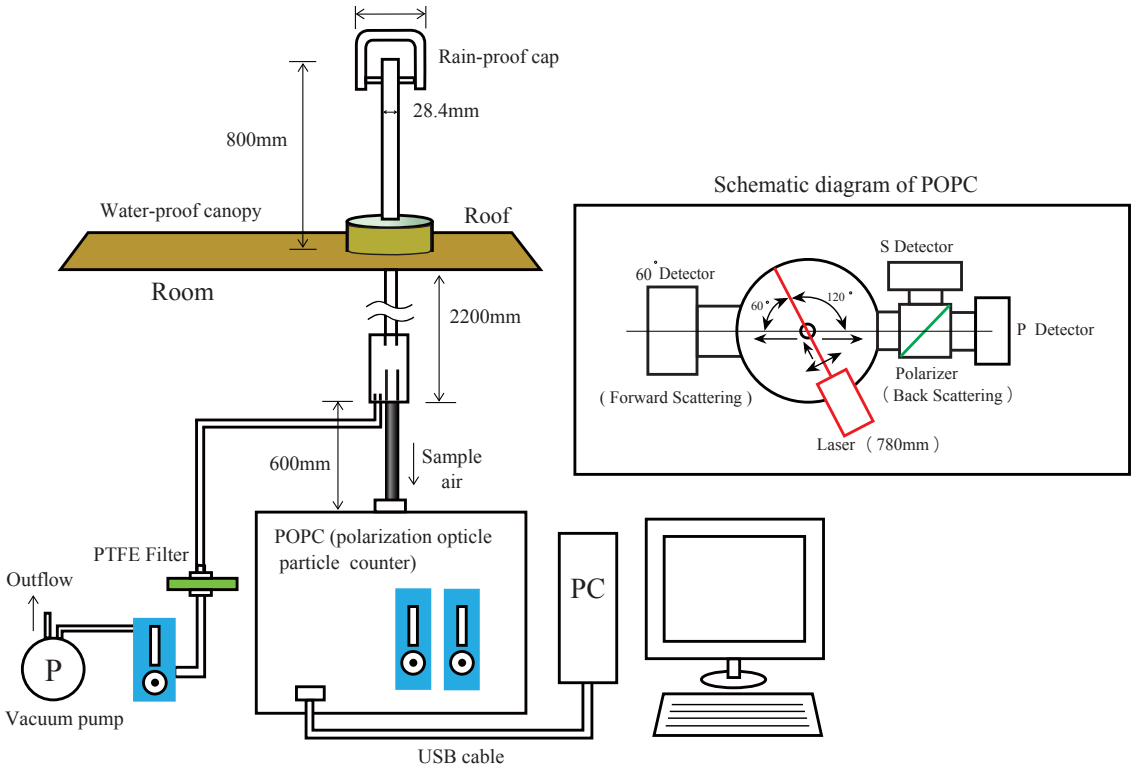

Fig. 4 Schematic diagram of the polarization optical particle counter (POPC) instrument and the layout of air sampling lines.

S/[S+P]) is a good indicator of particle sphericity because the direction of polarization of scattered light for spherical particles is identical to that of the incident light, whereas it increased significantly for nonspherical particles (e.g., dust). The mass concentration is calculated by assuming particle weights appropriate for specific particles. The overall measurement uncertainty in the number density of supermicron particles is less than 15%. Details of the POPC have previously been reported [29].

2.5 Multiangle absorption photometry

Observations of black carbon (BC) were used to distinguish domestic from transboundary air pollution. BC was observed using a multiangle absorption photometer (MAAP; MAAP5012; Thermo Fisher Scientific, Waltham, MA, USA) from the top of a two-story building of RIAM (the same location as the POPC measurement) from September 2014 to July 2016.

2.6 CO gas measurement

CO is an important pollutant tracer for both LRT and domestic emissions. CO measurements (Thermo Model 48) were conducted from the top of a two-story building of RIAM (the same location as the POPC measurement) from September 2014 to March 2016.

3. Results and Discussion

3.1 Synoptic conditions and dust events during observation period

Daily mean and maximum wind speeds (WS), daily mean temperature (T), relative humidity (RH), and precipitation in Fukuoka, as observed by the Japan Meteorological Agency, are shown in Figs. 5a and 5b. It is well known that the Japanese climate is controlled by changes in Asian monsoons. During the summer monsoon (characterized by SSE winds from the hot and moist air masses of the Pacific High), air temperatures and RH are at their maximum, whereas during the winter monsoon (characterized by a NNW continental cold air outflow), low temperatures and reduced precipitation are observed in Fukuoka. Maximum wind speeds in excess of 10 m s^{-1} in summer and fall indicate the effects of typhoons (Fig. 5a). The difference in precipitation between August 2014 and August 2015 is important for examining differences in the NH_3 concentration, where August 2014 had more rainfall than August 2015. PM_c measured by the ACSA-12 and POPC observations of coarse particles (diameter 3.6–6 μm) showed significant onsets of dust, denoted by the labels A–G in Fig. 5e. Details of these dust events have been reported in literatures [17–19].

3.2 Variation by time in aerosols and related trace gases

Figs. 5c–5g shows the daily mean of $PM_{2.5}$, PM_c, POPC in coarse particles (diameter 3.6–6 μm), BC, and CO. Figs. 6a–6f shows the daily mean concentration of fSO_4, NH_3, fNH_4^+, HNO_3 by denuder, $fNO3^-$, and cNO_3^-. Fig. 7 shows the monthly mean (a) $PM_{2.5}$, (b) fine- and coarse-mode SO_4^{2-}, (c) fine- and coarse-mode NH_4^+, (d) NH_3, (e) CO, and (f) OBC in the form of box-and-whisker plots (10th, 25th, 50th, 75th, and 90th percentile values are marked). Monthly mean of coarse mode aerosols are shown by the dashed line (Figs. 7b and 7c). Fig. 8 shows the monthly average (a) HNO_3, (b) total NO_3, (c) coarse NO_3^-, and (d) fine NO_3^- levels.

3.2.1 General overview

Concentrations of major aerosol components and trace gases demonstrated clear seasonal variabilities, as shown in Figs. 5–8. Monthly variation in mass concentrations of $PM_{2.5}$ shows a bimodal distribution, with peaks during spring and winter, and minimum concentrations were observed in the summer (Figs. 5 and 7). PM_c concentrations shows a pronounced peak in the spring due to the frequent impacts of dust events (Figs. 5d and 5e). The high correlation between $PM_{2.5}$ and fSO_4 ($PM_{2.5}$ = 2.87 × fSO_4 + 4.24; unit = μg m^{-3}; R = 0.84) suggests that the variation in $PM_{2.5}$ was driven mainly by fSO_4^{2-}, a major component of $PM_{2.5}$. The mass concentration of fSO_4^{2-} (Fig. 6b) showed two peaks during January and June, and SO_4^{2-} peaks were observed intermittently in colder seasons.

High SO_4^{2-} levels in the winter depended on the frequency of long-range transport (LRT) from the Asian continent, but the maximum concentration in summer suggests that the conversion of SO_2 to sulfate played a vital role in tropospheric aerosol loading over East Asia. This was also related to meteorological conditions, i.e., the high RH in summer. Mass concentration of cSO_4^{2-} was about 0.1–0.2 times the value of fine SO_4^{2-} (monthly average relationship: cSO_4^{2-} = 0.185 × fSO_4^{2-} – 0.052; unit = μg m^{-3}; R = 0.66). The increase in cSO_4^{2-} during winter cannot be neglected in the analysis of the SO_x mass budget.

The concentrations of BC and CO showed winter maxima and summer minima, which suggests that seasonal anthropogenic emissions were a major contribution (Figs. 7e and 7f). Linear regression of these data yielded CO (ppb) = 138.3 OBC (μg m^{-3}) + 202.85 (R = 0.61).

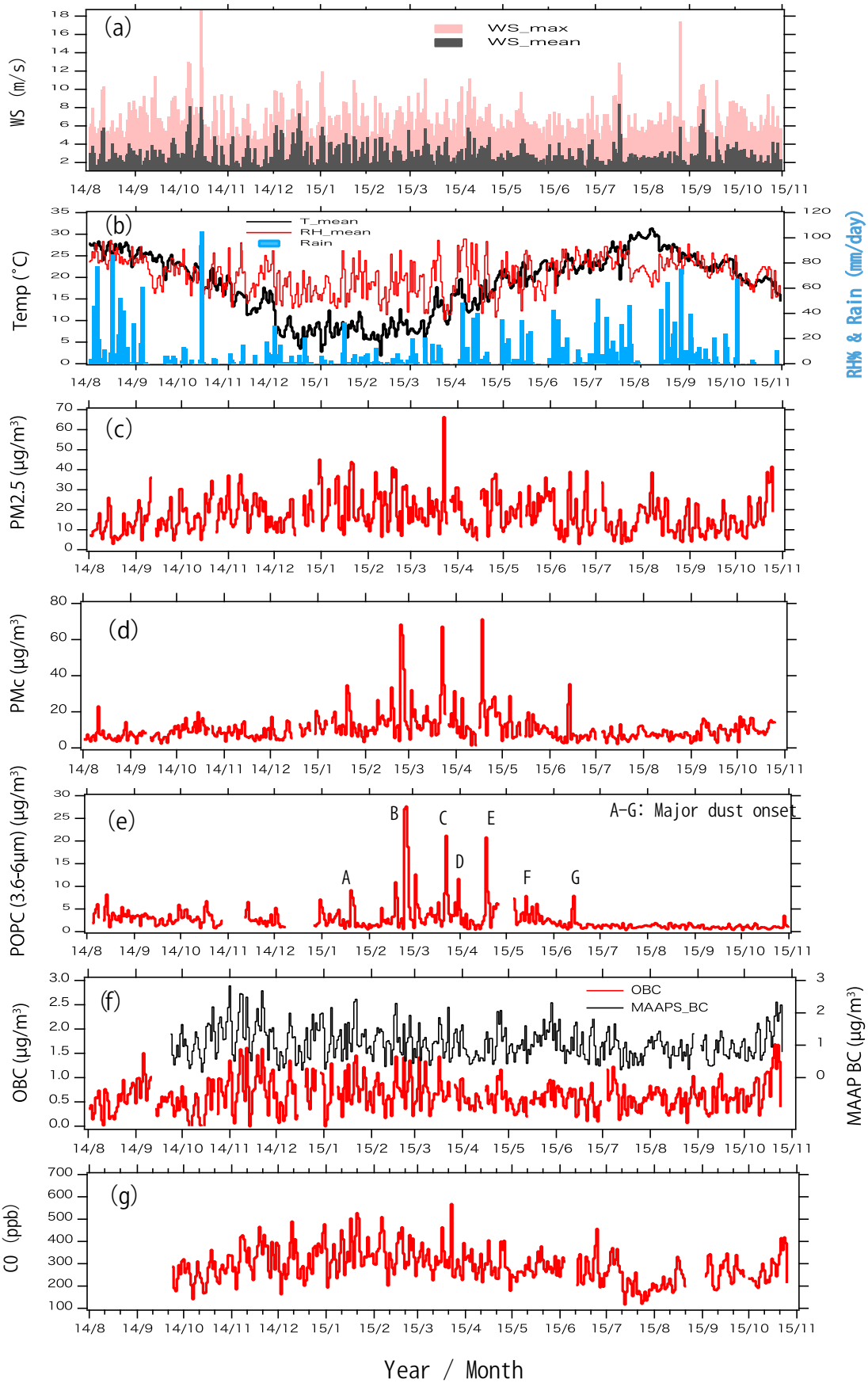

Fig. 5 Daily average variation by time in (a) WS, (b) temperature, RH, rainfall, (c) $PM_{2.5}$, (d) PM_c, (e) particles between 3.6 and 6 μm by POPC, (f) BC and (g) CO.

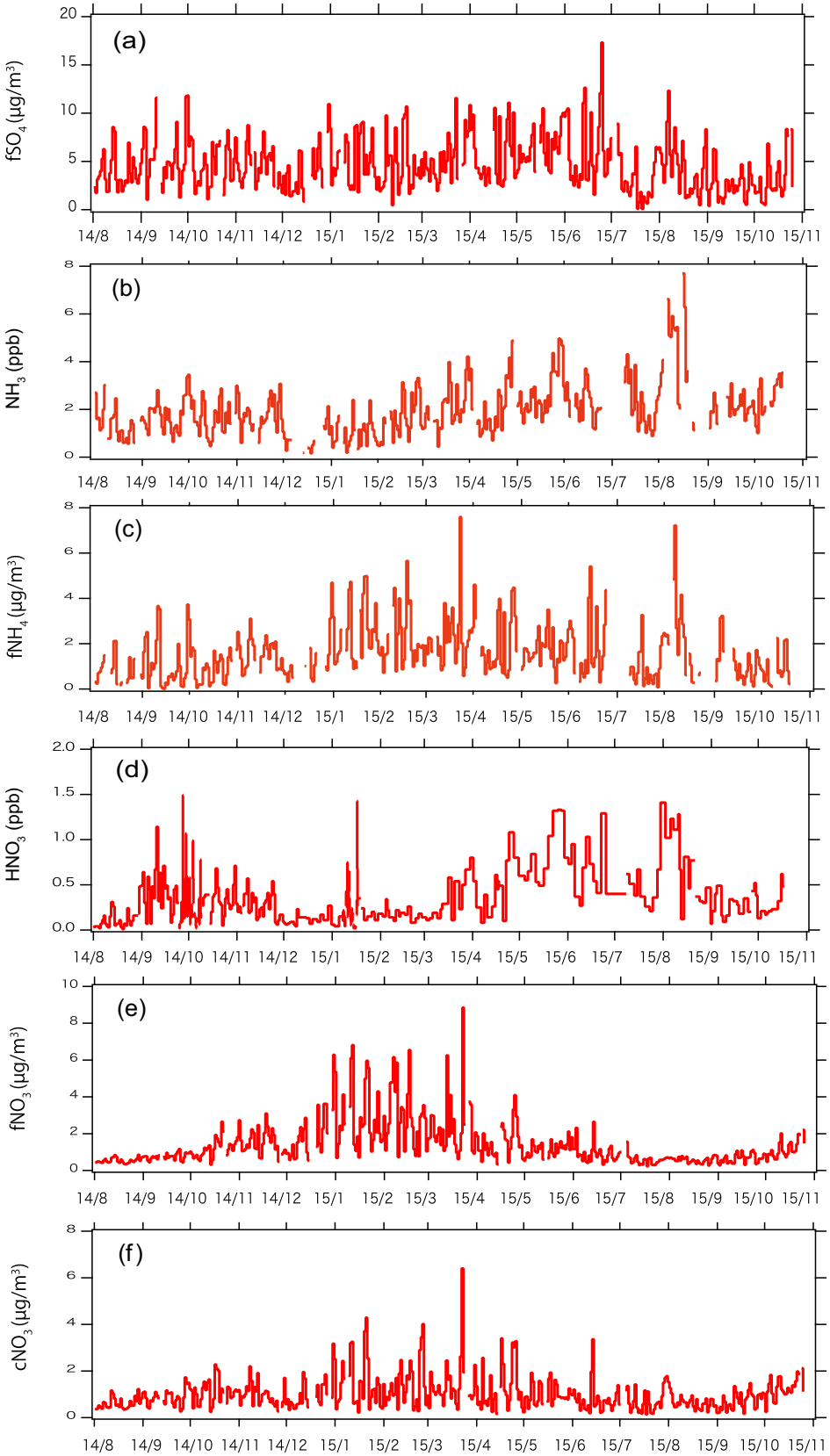

Fig. 6. Daily average variation by time in (a) fSO_4^{2-}, (b) NH_3, (c) fine NH_4^+, (d) HNO_3, (e) fine NO_3^-, and (f) coarse NO_3^-.

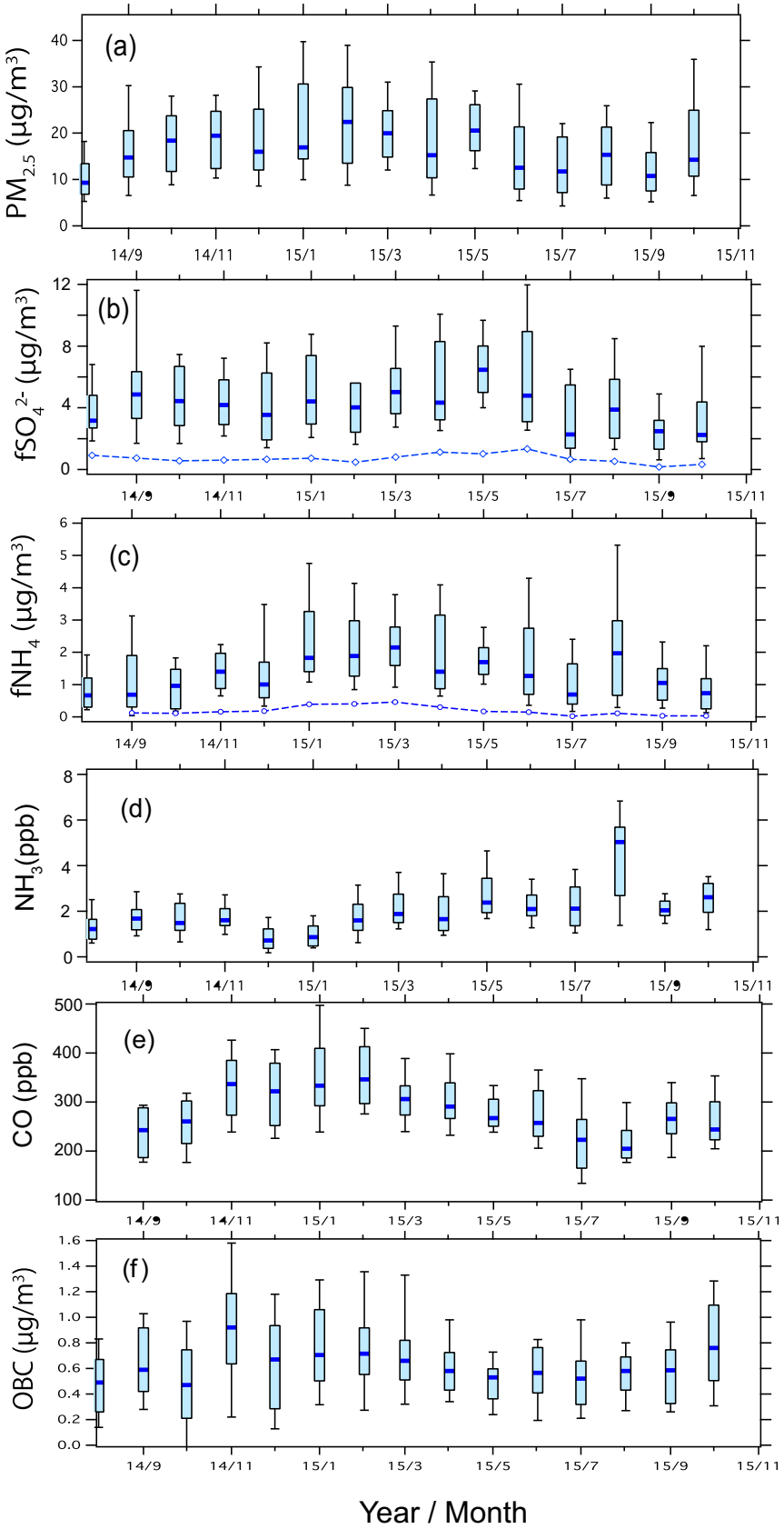

Fig. 7. Monthly average box-and-whisker plots (10th, 25th, 50th, 75th, 90th percentile values) of (a) $PM_{2.5}$, (b) fine SO_4^{2-}, (c) fine NH_4^+, (d) NH_3 gas, (e) CO, and (f) OBC. The blue lines in (b) and (c) show the ACSA-observed coarse-mode concentrations.

Mass concentration of NO_3^- levels was higher during the winter and lower in the summer, exhibiting clear seasonal changes. The mean value of fNO_3^- in winter was 2.62 ± 1.64 μg m^{-3}. The daily maximum was 6–9 μg m^{-3} and it was sometimes higher than SO_4^{2-}, where the peaks occurred at the same times as SO_4^{2-}. This indicates that fNO_3^- was also controlled by LRT from the Asian continent [14]. In the summer, fNO_3^- was small because the (RH-dependent) equilibrium between NH_4NO_3, NH_3, and HNO_3 shifts toward the gas-phase species under warm conditions. The monthly mean fNO_3^- from June to September was 0.68 ± 0.34 μg m^{-3}. The coarse-mode NO_3^- showed distinct peaks during the dust events (marked A–G in Fig. 5e), which indicates the formation of coarse dust nitrate during transport [19].

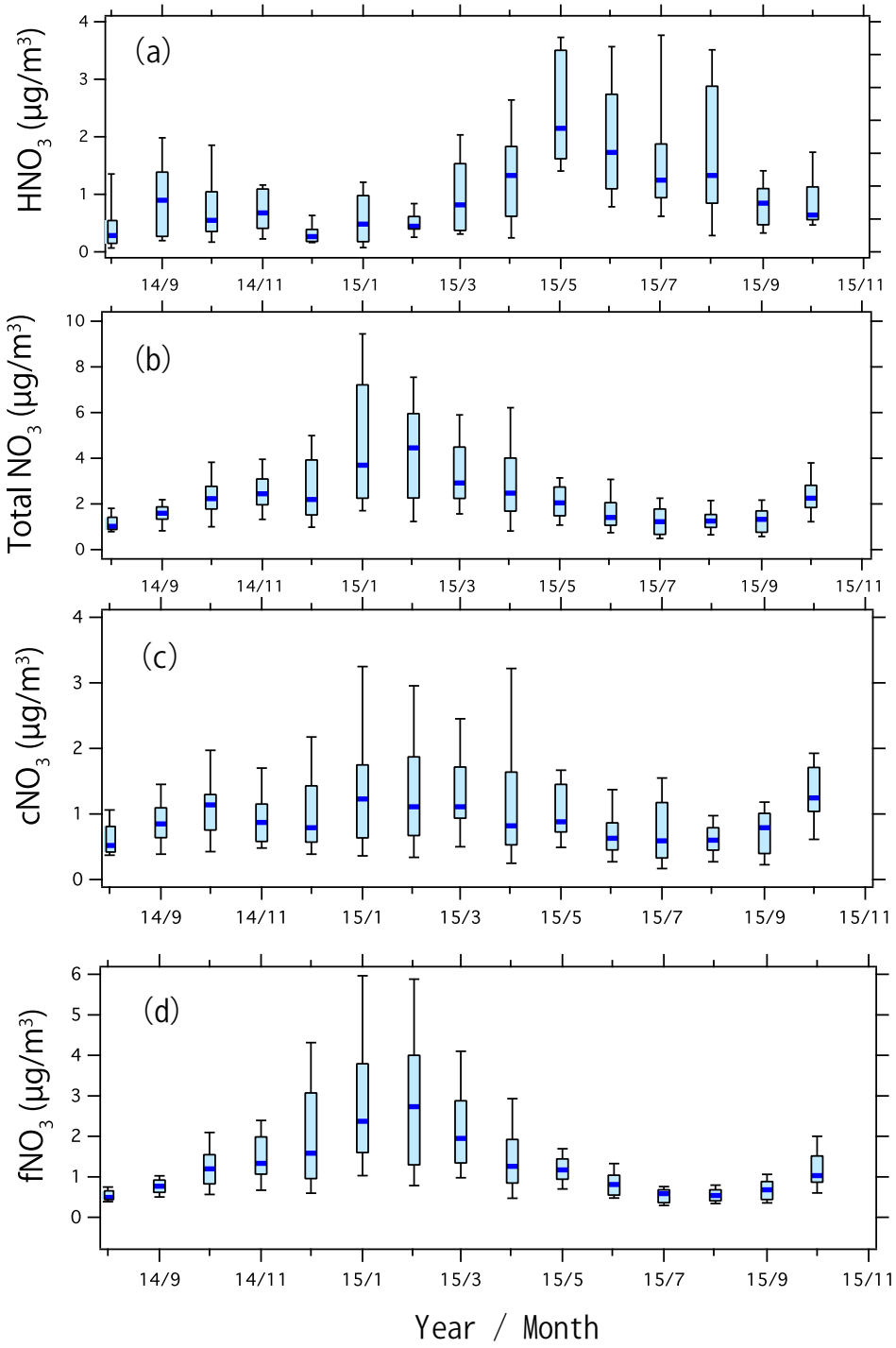

Fig. 8 Monthly average box-and-whisker plots (10th, 25th, 50th, 75th, 90th percentile values) of (a) HNO_3, (b) total NO_3, (c) coarse NO_3^-, and (d) fine NO_3^-.

3.2.2 Diurnal variation by season

Diurnal variations in temperature, WS, RH, precipitation, mass concentration of $PM_{2.5}$, PM_c, fSO_4^{2-}, fNO_3^-, fNH_4^+, NH_3, BC, and CO in different seasons (SON, DJF, MAM, JJA) during the observation period are illustrated in Fig. 9. Numbers in the upper right of each frame correspond to the arithmetic mean of observations from each season.

As expected, the mass concentrations of $PM_{2.5}$ and fSO_4^{2-} did not show evident diurnal trends (Fig. 9, d1–d4 and f1–f4), which suggests that local formation was only a minor contributor to mass concentrations in the Fukuoka area. The mean concentrations of $PM_{2.5}$ were 17.9 μg m^{-3}, 20.6 μg m^{-3}, 20.5 μg m^{-3}, and 15.1 μg m^{-3} in autumn, winter, spring, and summer, respectively. The mean concentration of fSO_4^{2-} was 4.5–5.9 μg m^{-3}. The mass concentration of PM_c showed a

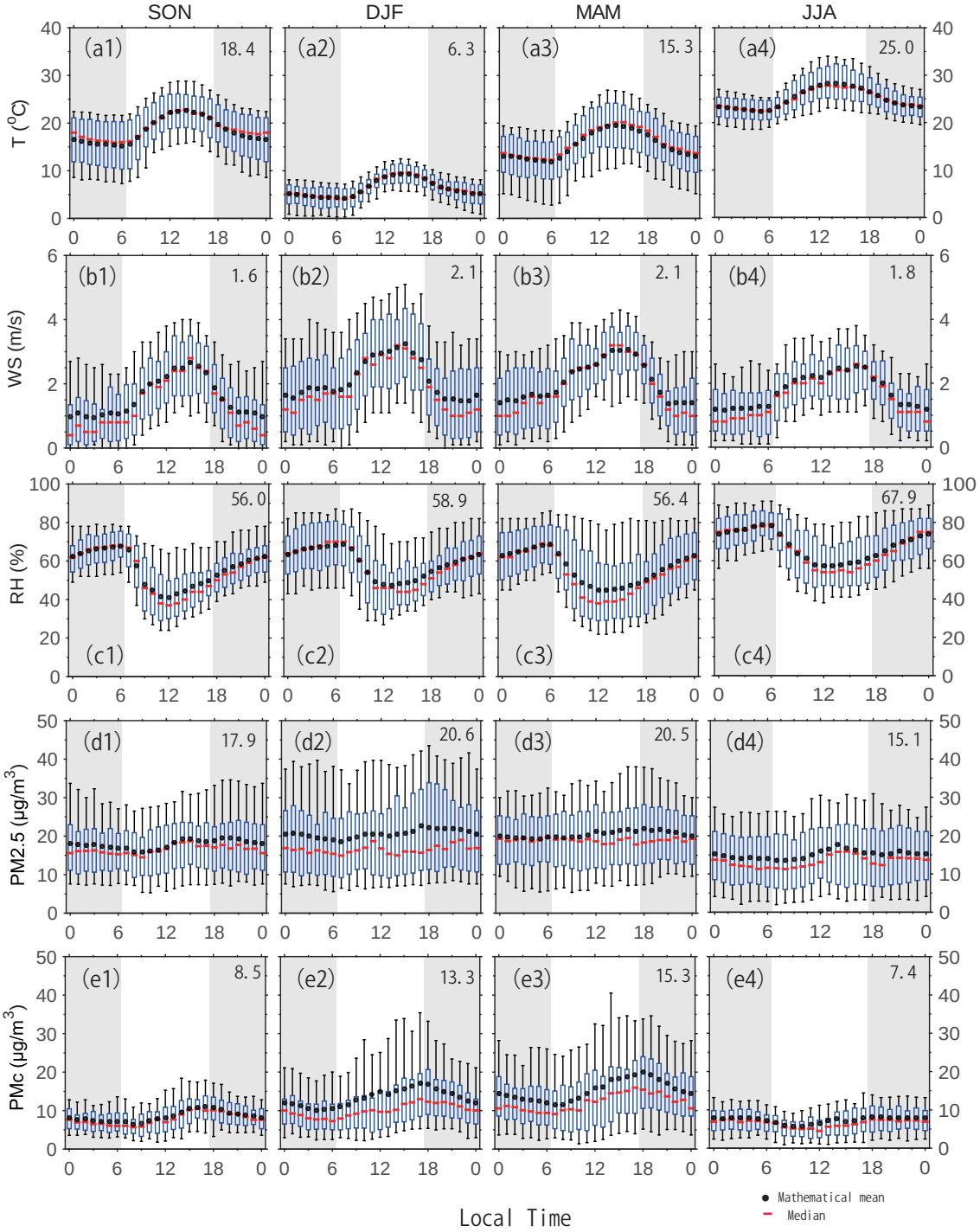

Fig. 9. Diurnal variation in temperature, WS, RH, $PM_{2.5}$, and PM_c for different seasons (September 2014–August 2015). The number in each frame indicates the average value.

daytime-high and nighttime-low pattern (Fig. 9, e1–e4), which could be attributed in part to anthropogenic activities. In addition, the observation site was located 12.8 km south of the Hakata-Bey (Genkai Nada) coastal area, and the wind speed normally reached its peak at noon because of both topographic effects and land-sea breeze circulation (Fig. 9b). Therefore, the corresponding transport of sea salt contributed to the mass in coarse mode. No clear increase in coarse-mode particles was observed during the summertime (Fig. 9, e4) because of frequent precipitation and the elevated dry deposition velocities of large particles under high RH conditions in a deep planetary boundary layer (PBL).

The mass concentration of fNO_3^- showed weak diurnal trends during the spring and winter (Fig. 9, g3 and g2). The peak appeared at 1000 JST (near rush hour) and reflected the domestic formation of nitrate due to local emissions of NO_x. However, the arithmetic mean of fNO_3^- was higher than the median value during winter and spring, which indicates that fNO_3^- was strongly impacted by sporadic high concentration pollutants due to LRT from outside Japan. Mass concentrations of fNO_3^- during the summer were generally less than 1.0 μg m^{-3} throughout the day, mostly owing to the gas–aerosol equilibrium toward gas-phase species under high-temperature conditions.

BC and CO (Fig. 9h and 9i) showed a pronounced peak during rush hour in the morning because of vehicle emissions

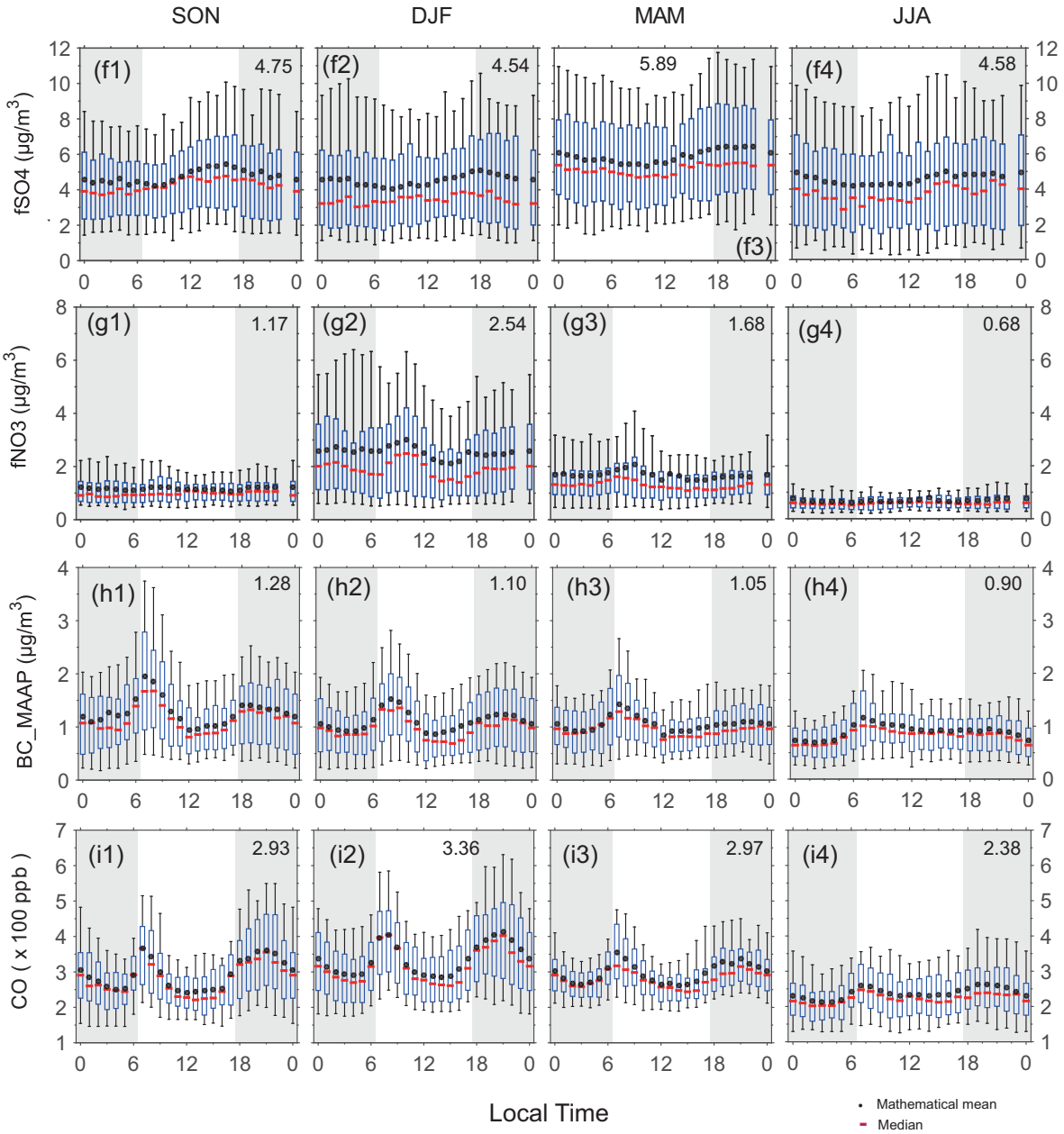

Fig. 9 (cont.) Diurnal variation in fSO_4^{2-}, fNO_3^-, BC by MAAP and CO for different seasons (September 2014–August 2015). The number in each frame indicates the average value.

and gradually decreased to their minimum at 1500 JST in the afternoon after full development of the PBL. The peak in the evening was due to rush hour traffic emissions and the shallow PBL after sunset (particularly SON and DJF). It is interesting that the evening CO peak was more pronounced than that of BC, which indicates differences in the emitters of BC and CO.

The mean mass concentrations of NH_3 (Fig. 9j) show a clear seasonal cycle, with values of 1.64 μg m^{-3}, 2.01 μg m^{-3}, 1.20 μg m^{-3}, and 0.86 μg m^{-3} for spring, summer, autumn, and winter, respectively. This seasonal cycle was very similar to that of the ambient temperature. Peak values appeared around 0900–1000 local time, with no peaks in the evening. The timing of the NH_3 peak was delayed around 2–3 h from the CO peak, which indicates that its major contributors were different from those of CO and BC.

The gas–aerosol partitioning between NH_3 and NH_4^+ was also investigated. Fig. 9m shows the gas fractions; this peaked in the summer at 63% and reached a winter minimum of 31%. The mean values of NH_4^+ (Fig. 9k) also show a clear seasonal cycle (anticorrelated with NH_3), with values of 1.86 μg m^{-3}, 1.51 μg m^{-3}, 1.11 μg m^{-3}, and 2.00 μg m^{-3} for spring, summer, autumn, and winter, respectively. One of the counter-ions of NH_4^+ is SO_4^{2-}, which does not show evident diurnal variability (Fig. 9f), and we also found a reasonable correlation between NH_4^+ and NO_3^-.

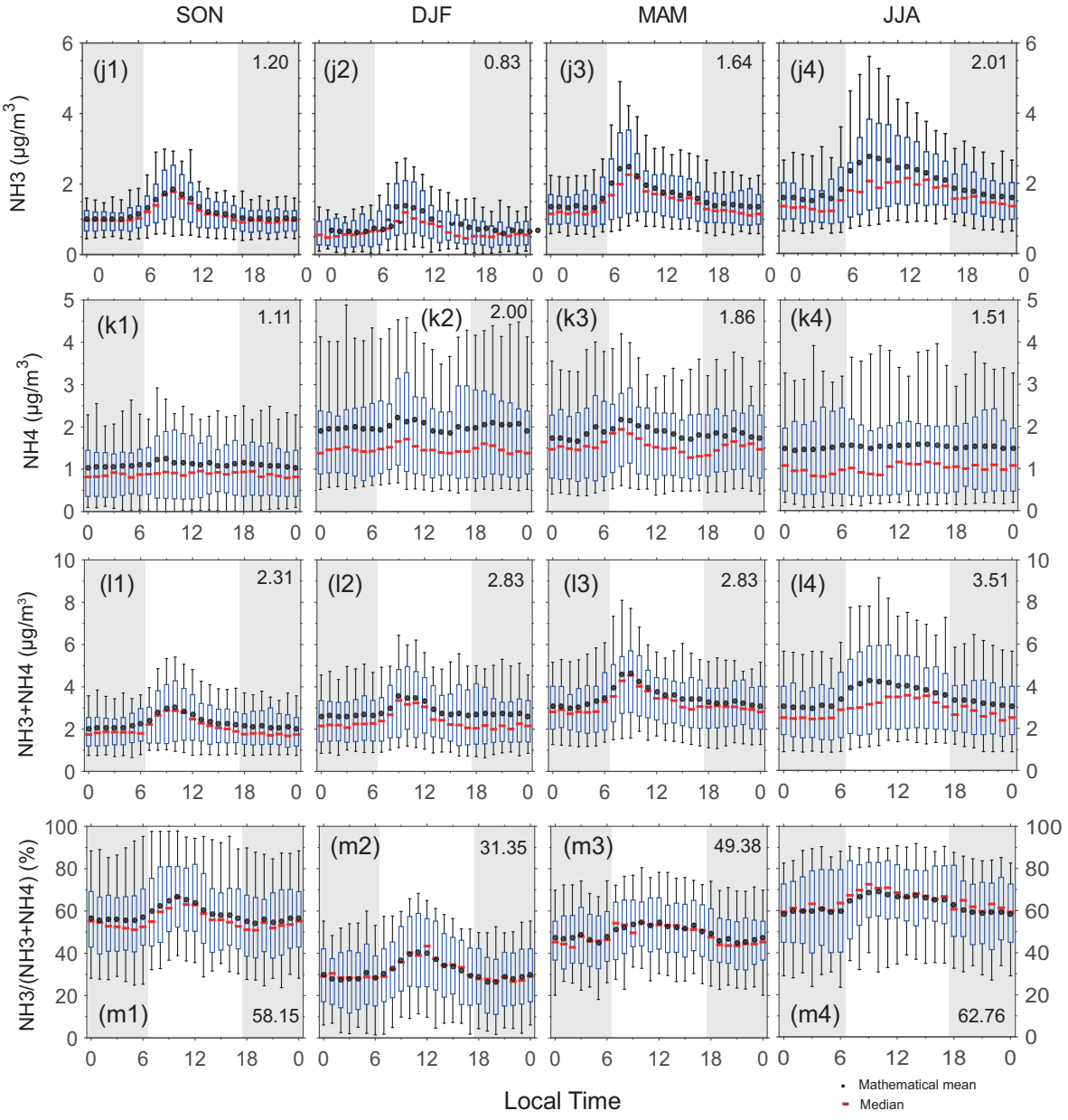

Fig. 9 (cont.) Diurnal variation in NH_3, NH_4^+, NH_3+NH_4^+, and NH_3 gas fraction for different seasons (September 2014–August 2015). The number in each frame indicates the average value.

3.2.3 Weekday and weekend differences: Local contributions

Fig. 10 shows the diurnal variation in CO, BC, NH_3, and NH_4^+ between cold and warm seasons as well as weekday and weekend periods. The concentrations of CO and BC in Fukuoka city reached their peaks when anthropogenic activities were intensive, in particular during rush hour (0700–0800 JST, particularly in cold seasons). The mixing ratios of CO during rush hour on weekdays showed mean values of 300 and 400 ppb in warm and cold seasons, respectively, higher than the 280 ppb (warm season) and 350 ppb (cold seasons) on the weekends (Fig. 10a).

Mass concentrations of BC during rush hour in the warm (cold) seasons were 1.27 μg m^{-3} (1.77 μg m^{-3}) and 1.14 μg m^{-3} (1.42 μg m^{-3}) for weekdays and weekends, respectively (Fig. 10b). The moderate increase in CO and BC during the warm seasons at night was due to the fact that the PBL height was still high at that time, whereas the sharp nighttime increase observed in the cold seasons was due to the rapid development of a stable boundary layer.

The corresponding profiles for NH_3 showed significant differences from CO. The timing of the NH_3 peak was 2–3 h later than that of CO, which indicates that traffic activities did not have a strong impact on NH_3 emissions. NH_3 did not exhibit an evening peak in all the seasons, and did not show clear differences at weekday and weekend. The high NH_3 concentrations may have been influenced by emissions from local agriculture and poultry farming 5–10 km south of the observation site (see Fig. 1), which is strongly dependent on the ambient temperature.

It is interesting to note that NH_3 was higher on weekends than on weekdays during warm seasons, unexpectedly. We found that total NH_x (NH_3 + NH_4^+) was the same on weekdays and weekends during the warm season, which indicates that more NH_3 converts to NH_4^+ on weekdays because of higher SO_2 and NO_x emissions. However, during cold seasons, we observed many dust events and LRT episodes (which may occur at any time in the week), and so we cannot find a consistent explanation in this case.

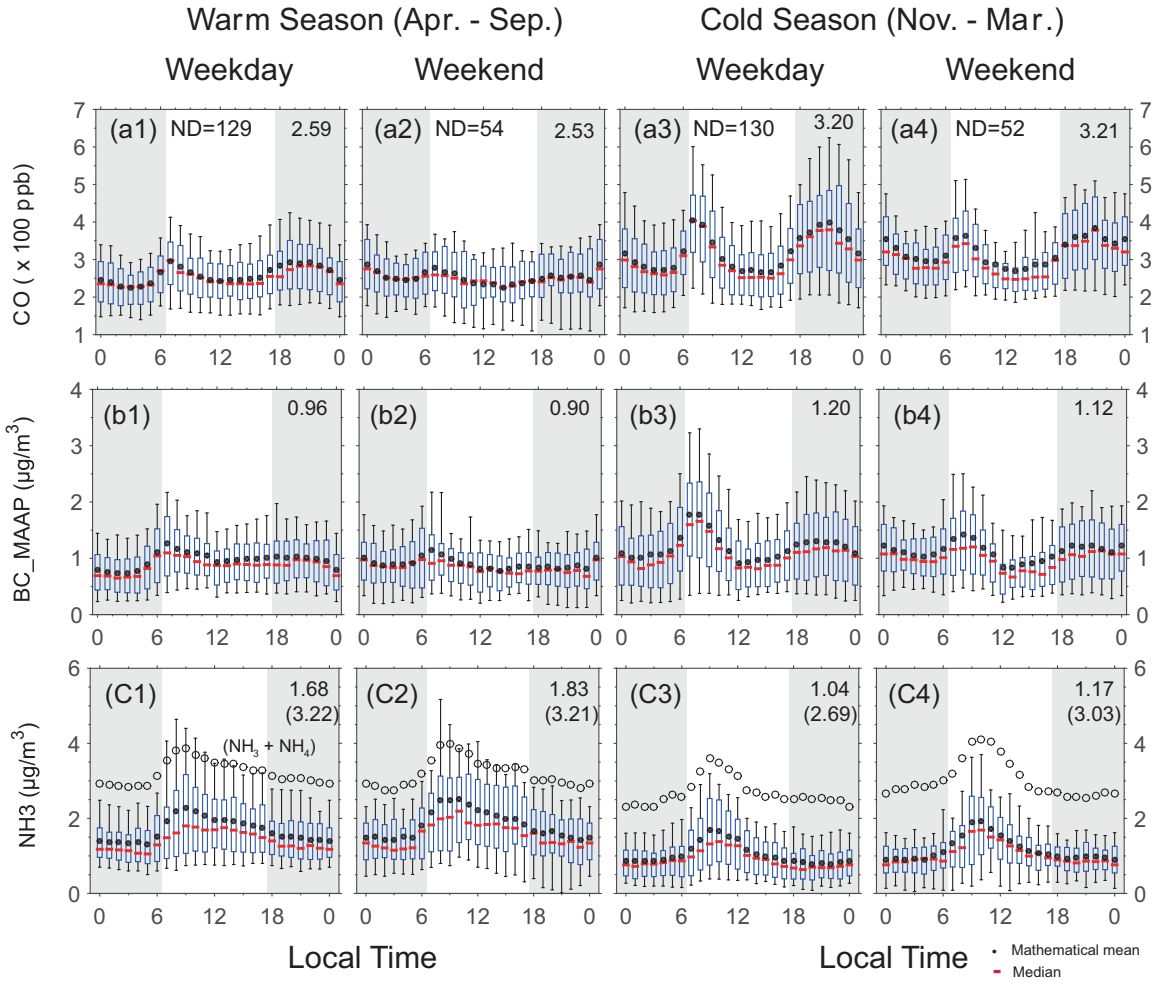

Fig. 10 Weekday and weekend diurnal variation in CO, BC, and NH_3 for warm seasons (April–September) and cold seasons (November–March). The number in each frame indicates the average value. In (c), the open circles represent NH_x (NH_3 + NH_4^+), and average values are given in parentheses.

3.2.4 Diurnal variation on days with and without precipitation

Fig. 11 compares the diurnal variation in CO, BC, NH_3 $PM_{2.5}$, and PM_c between 2-day continuous periods without and with precipitation for only warm seasons (April to September). We found that mixing ratio of CO exhibited almost no differences between days with and without precipitation, which indicates that anthropogenic CO emissions was not influenced by precipitation, and the effect of wet scavenging were negligible.

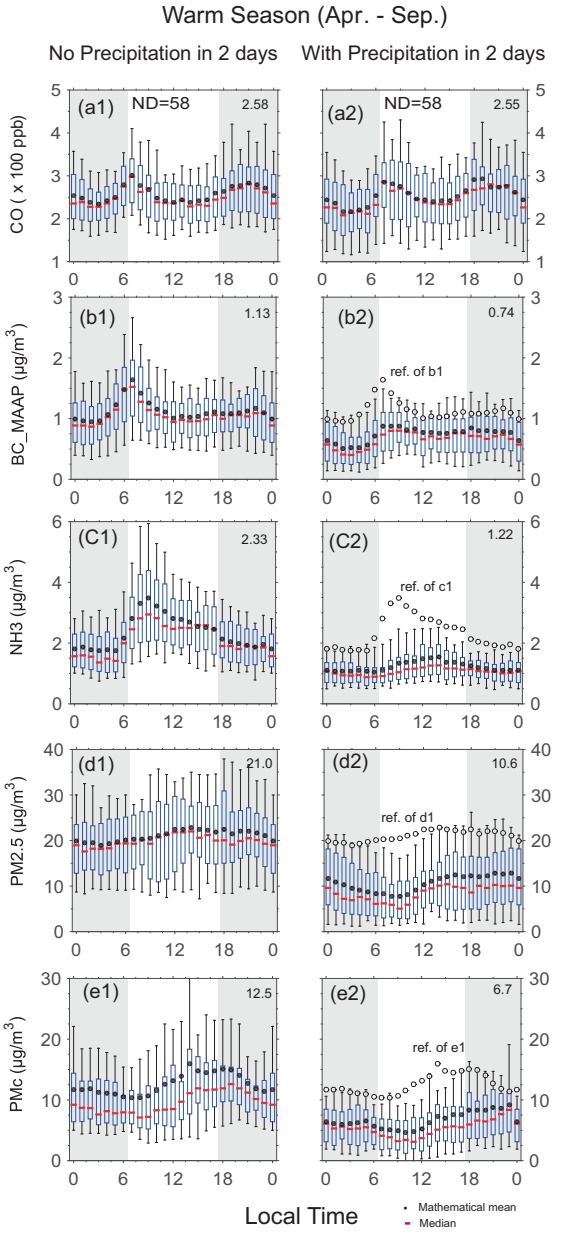

Fig. 11 Diurnal variation in CO, BC, NH_3, $PM_{2.5}$, and PM_c, for warm seasons with and without precipitation days. The number in each frame indicates the average value. In (b–e), the open circles represent the reference case (without precipitation, from the left figures).

Mass concentration of BC was higher on the days without precipitation than those days with precipitation, implying that they were washed out during the rain, even if the particle diameter of BC was small,. BC emissions from open burning may be less on rainy days. NH_3 concentrations showed large differences of almost a factor of 2. These differences may arise from changes in emissions (i.e., high emissions on dry days) and washout processes, because it has a high solubility in water.

$PM_{2.5}$ and PM_c exhibited similar variation pattern, with higher values in the afternoon due to transport (by northerly sea breeze) from downtown Fukuoka to the Chikushi Campus area. Both were higher on days without precipitation because of the relatively stronger local dust emissions and sea salt transport on days without precipitation. $PM_{2.5}$ and PM_c washout efficiencies (about 50%) were larger than those for BC (35%), because washout efficiency is a function of aerosol size; BC has a smaller size and thus a smaller washout efficiency.

3.3 Monthly variation in total NO_3 and NH_x

Fig. 12 shows the observed monthly variation in (a) NH_x (NH_3, fNH_4^+, cNH_4^+), (b) total NO_3 (HNO_3, fNO_3^-, cNO_3^-), and (c and d) the relative mass fraction of NH_x and NO_3. This figure clearly shows the highest mass concentrations of fNO_3^- in winter, whereas HNO_3 increased in summer, accounting for 30–40% of total NO_3; this was due to changes in the thermal equilibrium of gases and particles. Note that cNO_3^- was always higher than fNO_3^-, where cNO_3^- made up 27–55% of the total NO_3 and exceeded 45% in winter. We observed 0.5–1.0 μg m^{-3} (0.2–0.4 ppb) HNO_3, even during winter.

The observations showed that fNH_4^+ was higher throughout the year, and NH_3 levels were also high, even in winter. The high NH_3 concentrations may have been influenced by local agriculture and poultry farming 5–10 km south of the observation site. The high NH_3 concentration (see Fig. 6b) in August 2015 (4 times higher than in August 2014) was due to differences in temperature and precipitation (not shown in Fig. 12 because coarse-mode aerosol measurements started in September). The NH_3 concentration in August 2015 was significantly higher than in July and September; however, the NH_3 fraction of total NH_x was similar over the 3 months, which may have been because of high SO_2 emissions from volcanoes such that more $(NH_4)_2SO_4$ was formed in August [30]. In addition, fNO_3^- was higher in August than in July because higher precursors (both NH_3 and HNO_3) enhanced the formation of NH_4NO_3. The annual average cNH_4^+/total NH_x ratio was 10% but increased to 15% in winter (JFM). This indicates that the cNH_4^+ component in winter is important for understanding the behavior of cNO_3^- and cSO_4^{2-}.

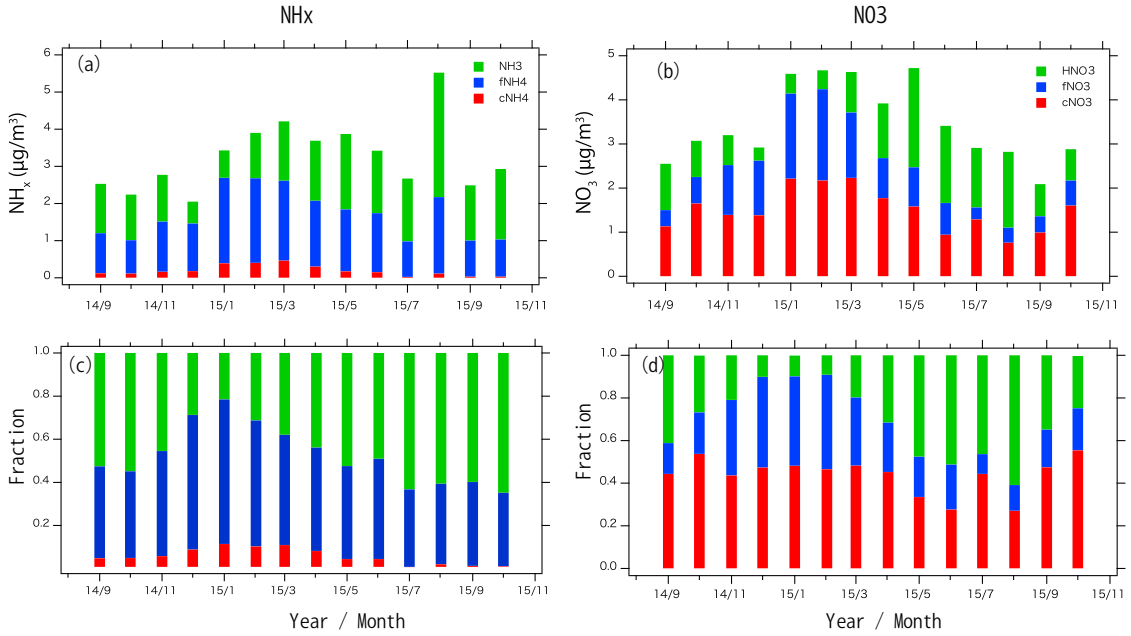

Fig. 12 Monthly average values of (a) NH_x (NH_3, fNH_4^+, cNH_4^+) and (b) NO_3, (HNO_3, fNO_3^-, cNO_3^-). Panels (c) and (d) show the mass fractions (%) of NH_x and total NO_3 observed by the D-F pack method.

4. Concluding Remarks

Long-term simultaneous observation data on aerosol chemical compositions in both fine- and coarse-mode were analyzed at 1 h intervals around the Chikushi Campus of Kyushu University, Fukuoka (33.52°N, 130.47°E) from August 2014 to October 2015. Detailed analyses of observational data were performed to better understand the seasonal variation in $PM_{2.5}$-related aerosol components and trace gases and the impact of long-range transport from the Asian continent.

The continuous measurement of SO_4^{2-}, NO_3^-, BC, OC with the ACSA-12 monitor, and NH_4^+ and NH_3 with the MF-NH_3A instrument, in addition to D-F pack/IC analysis, has established a long-term simultaneous fine- and coarse-mode aerosol and gas data set for Fukuoka, Japan.

Daily and monthly mean aerosol concentrations of aerosol were analyzed to show the general seasonal variation in pollution. We found that fine aerosols (fSO_4^{2-}, fNO_3^-, and fNH_4^+) explained most of the seasonal variability in $PM_{2.5}$. A newly developed POPC instrument was quite useful for detecting the onset of dust from the Asian continent; we found high concentrations of coarse-mode NO_3^- during the dust period, which indicates the formation of dust nitrate during transport [19].

We also analyzed diurnal variation in basic aerosol components for different seasons, differences between weekdays and weekends, and sensitivity to precipitation. We demonstrated that the mass concentrations of $PM_{2.5}$ and fSO_4^{2-} did not show any obvious diurnal variability, which suggests that local formation was only a minor contributor to ambient particle mass in the Fukuoka area. The median values of NH_3 showed a clear seasonal cycle that was very similar to that of the ambient temperature. Peak values of NH_3 appeared at around 9–10 local time, with no peak in the evening. The timing of the NH_3 peak was delayed around 2–3 h relative to the CO peak, which indicates that the main emitters of NH_3 were different from those of CO and BC.

The diurnal variation in CO, BC, NH_3, $PM_{2.5}$, and PM_c between continuous 2-day periods with and without precipitation during the warm season (April to September) shows that CO was not significantly affected by precipitation, although higher BC levels were observed on days without precipitation. $PM_{2.5}$ and PM_c showed similar variation by time, with higher values in the afternoon due to transport (by sea breeze) from downtown Fukuoka to the Chikushi Campus area. Both $PM_{2.5}$ and PM_c were higher on days without precipitation because of greater local dust and sea salt. NH_3 concentrations showed large differences of almost a factor of 2, which may result from differences in emissions (i.e., high emissions on dry days) and the high solubility of NH_3 in rain droplets.

Observational data for HNO_3, fNO_3^-, and cNO_3^- demonstrated that cNO_3^- accounted for the largest proportion of total nitrate (defined as the sum of fNO_3^-, cNO_3^-, and HNO_3), constituting 40–55% of total nitrate during the winter, whereas HNO_3 gas constituted approximately 40% of total nitrate in the summer and fNO_3^- peaked during the winter. This indicates the importance of coarse-mode NO_3^- measurements for mass budget studies of nitrate and numerical modeling of LRT.

Acknowledgments

This work was supported by a Grant-in-Aid for Scientific Research (JP25220101) from the Japan Society for the Promotion of Science (JSPS). This work was funded in part by the Collaborative Research Program of the Research Institute for Applied Mechanics, Kyushu University (No. 26AO-2, 27AO-6, 28AO-2). We thank Prof. H. Kobayashi of Yamanashi University for the operation of POPC. We also want to thank to Ms. M. Yamagami for NH_3 emission data processing used in Fig. 1, and Dr. Yukari Hara, Mr. Shuhei Kuwahara, and Mr. Yusuke Kamikuchi for performing D-F filter sampling at Kyushu University.

References

1) Lawrence, M.G., Lelieveld, J. Atmospheric pollutant outflow from southern Asia: a review. Atmospheric Chemistry and Physics, 10, 11017-11096, 2010
2) Zhang, X. Y. et al. Characterization of soil dust aerosol in China and its transport and distribution during 2001 ACE-Asia: 1. Network observations. Journal of Geophysical Research: Atmospheres, 108, 2003
3) Huebert, B.J., Bates, T., Russell, P.B., Shi, G.Y., Kim, Y.J., Kawamura, K., Carmichael, G. and Nakajima, T.. An overview of ACE-Asia: Strategies for quantifying the relationships between Asian aerosols and their climatic impacts. Journal of Geophysical Research-Atmosphere, 108, 2003
4) Seinfeld, J.H., Carmichael, G.R., Arimoto, R., Conant, W.C., Brechtel, F.J., Bates, T.S., Cahill, T.A., Clarke, A.D., Doherty, S.J., Flatau, P.J., Huebert, B.J., Kim, J., Markowicz, K.M., Quinn, P.K., Russell, L.M., Russell, P.B., Shimizu, A., Shinozuka, Y., Song, C.H., Tang, Y.H., Uno, I., Vogelmann, A.M., Weber, R.J., Woo, J.H. and Zhang, X.Y. Ace-Asia - regional climatic and atmospheric chemical effects of Asian dust and pollution. Bulletin of the American Meteorological Society, 85: 367-380, 2004
5) Jacob, D.J., Crawford, J.H., Kleb, M.M., Connors, V.S., Bendura, R.J., Raper, J.L., Sachse, G.W., Gille, J.C., Emmons, L. and Heald, C.L. Transport and chemical evolution over the Pacific (TRACE-P) aircraft mission: Design, execution, and first results. Journal of Geophysical Research-Atmospheres, 108, 2003
6) Carmichael, G.R., Tang, Y., Kurata, G., Uno, I., Streets, D., Woo, J.H., Huang, H., Yienger, J., Lefer, B., Shetter, R., Blake, D., Atlas, E., Fried, A., Apel, E., Eisele, F., Cantrell, C., Avery, M., Barrick, J., Sachse, G., Brune, W., Sandholm, S., Kondo, Y., Singh, H., Talbot, R., Bandy, A., Thorton, D., Clarke, A. and Heikes, B. Regional-scale chemical transport modeling in support of the analysis of observations obtained during the TRACE-P experiment. Journal of Geophysical Research-Atmospheres, 108, 2003
7) Uno, I., Yumimoto, K., Shimizu, A., Hara, Y., Sugimoto, N., Wang, Z., Liu, Z. and Winker, D.M. 3d structure of Asian dust transport revealed by Calipso Lidar and a 4dvar dust model. Geophysical Research Letters, 35, L06803, 2008
8) Itahashi, S., Yumimoto, K., Uno, I., Eguchi, K., Takemura, T., Hara, Y., Shimizu, A., Sugimoto, N. and Liu, Z. Structure of dust and air pollutant outflow over East Asia in the spring. Geophysical Research Letters 37, L20806, 2010
9) Li, J., Wang, Z.F., Zhuang, G., Luo, G., Sun, Y. and Wang, Q. Mixing of Asian mineral dust with anthropogenic pollutants over East Asia: A model case study of a super-duststorm in March 2010. Atmos. Chem. Phys. 12, 7591-7607, 2012
10) Uno, I., Sugimoto, N., Shimizu, A., Yumimoto, K., Hara, Y. and Wang, Z. Record heavy $PM_{2.5}$ air pollution over China in January 2013: Vertical and horizontal dimensions. SOLA, 10, 136-140, 2014
11) Wang, Z.F., Li, J., Wang, Z., Yang, W.Y., Tang, X., Ge, B.Z., Yan, P.Z., Zhu, L.L., Chen, X.S., Chen, H.S., Wand, W., Li, J.J., Liu, B., Wang, X.Y., Wand, W., Zhao, Y.L., Lu, N. and Su, D.B. Modeling study of regional severe hazes over mid-eastern China in January 2013 and its implications on pollution prevention and control. Sci. China-Earth Sci, 57, 3-13, 2014
12) Carmichael, G.R., Calori, G., Hayami, H., Uno, I., Cho, S.Y., Engardt, M., Kim, S.B., Ichikawa, Y., Ikeda, Y., Woo, J.H., Ueda, H. and Amann, M. The MICS-Asia study: Model intercomparison of long-range transport and sulfur deposition in East Asia. Atmospheric Environment, 36, 175-199, 2002
13) Itahashi, S., Uno, I., Hayami, H. and Fujita, S.-i. Modeling investigation of controlling factors in the increasing ratio of nitrate to non-seasalt sulfate in precipitation over Japan. Atmospheric Environment, 92, 171-177, 2014
14) Itahashi, S., Uno, I., Osada, K., Kamiguchi, Y., Yamamoto, S., Tamura, K., Wang, Z., Kurosaki, Y., Kanaya, Y. Nitrate transboundary heavy pollution over East Asia in winter, Atmos. Chem. Phys., 17, 3823-3843, 2017
15) Pan, X., Uno, I., Hara, Y., Kuribayashi, M., Kobayashi, H., Sugimoto, N., Yamamoto, S., Shimohara, T., Wang, Z. Observation of the simultaneous transport of Asian mineral dust aerosols with anthropogenic pollutants using a POPC during a long-lasting dust event in late spring 2014. Geophysical Research Letters, 42,

1593-1598, 2015

16) Pan, X., Uno, I., Hara, Y., Osada, K., Yamamoto, S., Wang, Z., Sugimoto, N., Kobayashi, H. and Wang, Z. Polarization properties of aerosol particles over western Japan: Classification, seasonal variation, and implications for air quality. Atmos. Chem. Phys. 16, 9863-9873, 2016
17) Uno, I., Yumimoto, K., Pan, X. L., Wang, Z., Osada, K., Itahashi, S., Yamamoto, S. Simultaneous dust–pollutants transport over East Asia: the Tripartite Environment Ministers Meeting March 2014 Case Study, SOLA, 13, 47-52, 2017
18) Uno, I., K. Yumimoto, K. Osada, Z. Wang, X.L. Pan, S. Itahashi and S. Yamamoto. Dust Acid Uptake Analysis during Long-lasting Dust and Pollution Episodes over East Asia based on Synergetic Observation and Chemical Transport Model, SOLA, 13, 109-113, 2017
19) Uno, I., K. Osada, K. Yumimoto, Z. Wang, S. Itahashi, X. Pan, Y. Hara, S. Yamamoto and T. Nishizawa. Importance of long-range nitrate transport based on long-term observation and modeling of dust and pollutants over East Asia, Aerosol and Air Quality Research, 17, 2017
20) Osada, K., T. Kamikuchi, S. Yamamoto, S. Kuwahara, X. Pan, Y. Hara, I. Uno. Comparison of ionic concentrations on size-segregated atmospheric aerosol particle based on a denuer-filter method and a Continuous Dichotomous Aerosol Chemical Speciation Analyzer (ACA-12), Earozoru Kenkyu, 31, 203–209, 2016 (in Japanese with English abstract)
21) Kannari, A., Tonooka, Y., Baba, T., Murano, K. Development of multiple-species 1km×1km resolution hourly basis emissions inventory for Japan, Atmos. Environ., 41, 3428-3439, 2007
22) Kimoto, H., Ueda, A., Tsujimoto, K., Mitani, Y., Toyasaki, Y. and Kimoto, T. Development of continuous dichotomous aerosol chemical speciation analyzer, Clean Technol., 23, 49–52, 2013 (in Japanese).
23) Osada, K., Ueda, S., Egashira, T., Takami, A., Kaneyasu, N. Measurement of gaseous NH_3 and particulate NH_4+ in the atmosphere by fluorescent detection after continuous air-water droplet sampling, Aerosol and Air Quality Research, 11, 170–178, 2011.
24) Genfa, Z., Dasgupta, P.K., Dong, S. Measurement of atmospheric ammonia. Environ. Sci. Technol., 23, 1467–1474, 1989
25) Perrino, C., Santis, F. D., Febo, A. Criteria for the Choice of a Denuder Sampling Technique Devoted to the Measurement of Atmospheric Nitrous and Nitric Acids, Atmos. Environ., 24, 617-626, 1990
26) Appel, B. R., Tokiwa, Y., Haik, M. Sampling of Nitrates in Ambient Air. Atmos. Environ., 15, 283-289, 1981
27) Vecchi, R., Valli, G., Fermo, P., D'Alessandro, A., Piazzalunga, A., Bernardoni, V. Organic and Inorganic Sampling Artefacts Assessment. Atmos. Environ., 43, 1713-1720, 2009
28) John,W., Hering, S., Reischl, G., Sasaki, G., Goren, S. Characteristics of Nuclepore Filters with Large pore size-II. Filtration Properties, Atmos. Environ., 17, 373-382, 1983
29) Kobayashi, H., M. Hayashi, K. Shiraishi, Y. Nakura, T. Enomoto, K. Miura, H. Takahashi, Y. Igarashi, H. Naoe, and N. Kaneyasu. Development of a polarization optical particle counter capable of aerosol type classification. Atmospheric Environment. 48. 486-492, 2014
30) Uno, I., Osada, K., Yumimoto, K., Wang, Z., Itahashi, S., Pan, X., Hara, Y., Kanaya, Y., Yamamoto, S., and Fiarlie, T. D. Seasonal variation of fine and coarse-mode nitrates and related aerosols over East Asia: Synergetic observations and chemical transport model analysis, Atmos. Chem. Phys. Discuss., in review, 2017